# Chapter 4 Relaxation Dynamics of CNDSB Nanobelts

4.1 Introduction

In previous section, we have report the relaxation dynamics of PPB and its nanoparticles by the using of field-emission scanning electron microscopy (SEM), femtosecond (fs) and picosecond (ps) time-solved spectroscopy, and X-ray diffraction (XRD).[1] With the same methods, we extend our work to its derivatives: (*Z*)-3-{4-[(*Z*)-2-cyano-2-phenyl-1-ethenyl]phenyl}-2-phenyl-2-propenenitrile(CN-DSB, the structure was shown in scheme 1).

Scheme 1
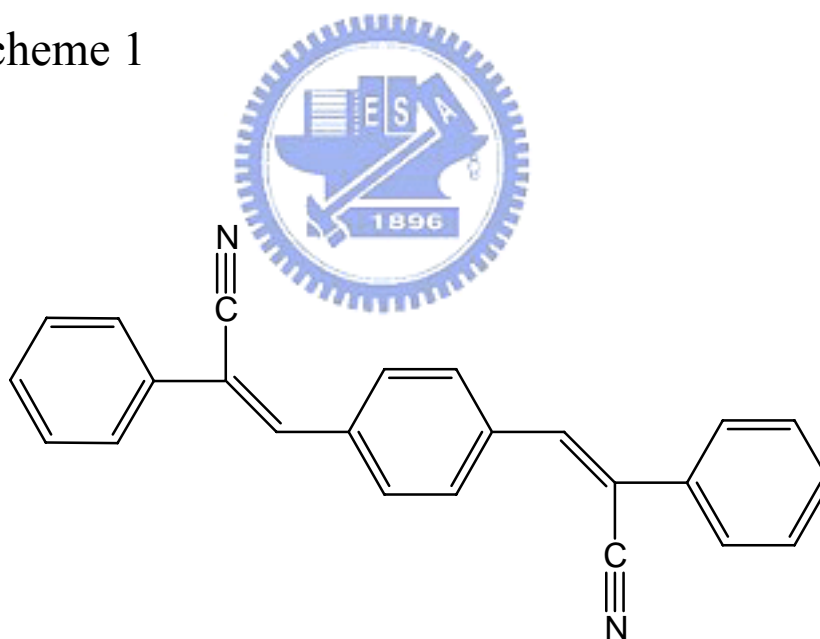
With the application of reprecipation method,[2] CNDSB form nanobelts as the volume fraction of water exceeds 70%. Like the case of PPB, CN-DSB itself is nonfluorescent and emitting strong fluorescence as it forms nanobelts. In this study

---

[1] Bhongale, C. J.; Chang, C. W.; Lee, C. S.; Diau, E. W. G.; Hsu, C. S. *J. Phys. Chem. B* **2005**, *109*, 13472

[2] Kasai, H.; Nalwa, H. S.; Oikawa, H.; Okada, S.; Matsuda, H.; Minami, N.; Kakuta, A.; Ono, K.; Mukoh, A.; H., N. *Jpn. J. Appl. Phys.* **1992**, *31*, 1132.

we measured the fluorescence lifetime of CN-DSB nanobelts and single crystal. The results indicate that two emissive states exist in those two conditions. We test the role of intramolecular motion by comparing the ps and fs time-resolved transients of CN-DSB in THF and Poly (methyl methacrylate) (PMMA). The result reveals that the intramolecular motion would lead to an efficient nonradiative channel, which caused the low quantum yield of CN-DSB THF solution. We also measure the fs time-resolved fluorescence decay of CN-DSB nanobelts in 80% water/THF solution. In CN-DSB nanobelts we observed a unique ultrafast decay, which was absent in PPB nanoparticles[1] , and the origin of this ultrafast decay will be discussed.

4.2 Experimental Section

Materials. CN-DSB was synthesized by Knoevenagel reaction.[3] Typically, KOH (4.2 g, 75.14 mmols) was added to a solution of terephthaladehyde (5.0 g, 37.20 mmol) and phenylacetonitrile (8.8 g, 75.14 mmol) in ethanol (50 mL). A greenish yellow gel-type mixture was formed immediately after addition. The resulting solution was stirred for overnight at room temperature. The mixture was then filtered and washed several times by ethanol. The crude power was recrystallized from chloroform to give greenish yellow solid (yield, 45%). ^{1}H NMR (300 MHz, CDCl$_3$): δ= 8.00 (s, 2H; Ar-H), 7.72-7.7.69 (m, 4H; Ar-H), 7.56 (s, 2H; Ar-H), 7.47-7.44 (m, 6H; Ar-H), 7.26 (s, 2H; vinyl); m.p. 270-272°C.

Formation of Nanostructures. CN-DSB nanostructures were obtained by a simple reprecipitation method. Water served as a precipitating solvent for CN-DSB in THF.

---

[3] Pond. S. J. K.; Rumi , M.; Levin, M. D.; Parker, T. C.; Beljonne, D.; Day, M. W.; Brédas, J.-L.; Marder, S. R.; and Perry. J. W. *J. Phys. Chem. A* **2002**, *106*, 11470.

Volume fractions of water were added up to 90%, with vigorous stirring at 296 K. Distilled water and THF were filtered with a membrane filter (pore size 0.2μm). In all samples, the concentration of chromophore (3.6×10^{-5} M) is kept at 3.6×10^{-5} M. To test the concentration effect on the formation of CN-DSB nanostructures, the sample with different concentrations, viz. 1.8×10^{-5} M, 3.6×10^{-5} M, and 7.2×10^{-5} M are prepared. These suspensions were homogenous and stable. Samples for SEM tests were prepared by dropping the sample mixture onto a microscopic glass or carbon tape and dried under vacuum.

Steady-state Spectral Measurements. ^{1}H NMR spectra were recorded (Unity-300 spectrometer at 300 MHz) in CDCl$_3$ solutions. Images were acquired on a field-emission scanning electron microscope (JSM-6500 F, JEOL); to enhance the conductivity of the specimen, a layer of platinum was sputtered for 30 s at a current 30mA and a pressure 4Pa. UV-visible absorption spectra (Hewlett-Packard HP8453 spectrometer) and fluorescence spectra (Hitachi F4500 spectrophotometer) were measured in standard manners.

4.3 Results and Discussion

4.3.1 Formation of CN-DSB Nanostructures

CN-DSB nanostructures in series volume fractions of water, viz. 0, 70, 80 and 90%, were prepared according to a simple reprecipitation method with THF as solvent and water as non-solvent. As the percentage of water was increased, because of the formation of nanostructures, the solution became milky. The shape of nanostructures

also changed from curvy nanoparticles (at 70%) to nanobelts (at 80 and 90%). Parts A, B and C in Figure 4.1 presents the SEM photographs of CN-DSB nanostructures obtained by varying the percentage of water in THF solution of CN-DSB. Although the aggregation of CN-DSB molecules might start at the early stages of mixing, well-evolved nanostructures only could be observed as the water volume fraction exceeding 70%. As the proportion of added water became greater than 70%, the molecules aggregated to larger structures, and the shape and size of CN-DSB nanostructures changed greatly giving rise to nanobelts. The formation of nanobelts is more or less similar to the case involving one-dimensional nanostructures of *p*-BSP in mixtures of water and THF.[4] Concentration dependence of the formation of CN-DSB nanostructures was also studied. The nanobelts suspensions were prepared at different concentrations, and the water percentage was controlled at 80%. The result indicates that with the increasing of concentration, only the size along the entire length of nanobelts increasing from 150 nm to 300 nm, and no other significant change is observed. (Figure 4.1D, B and E).

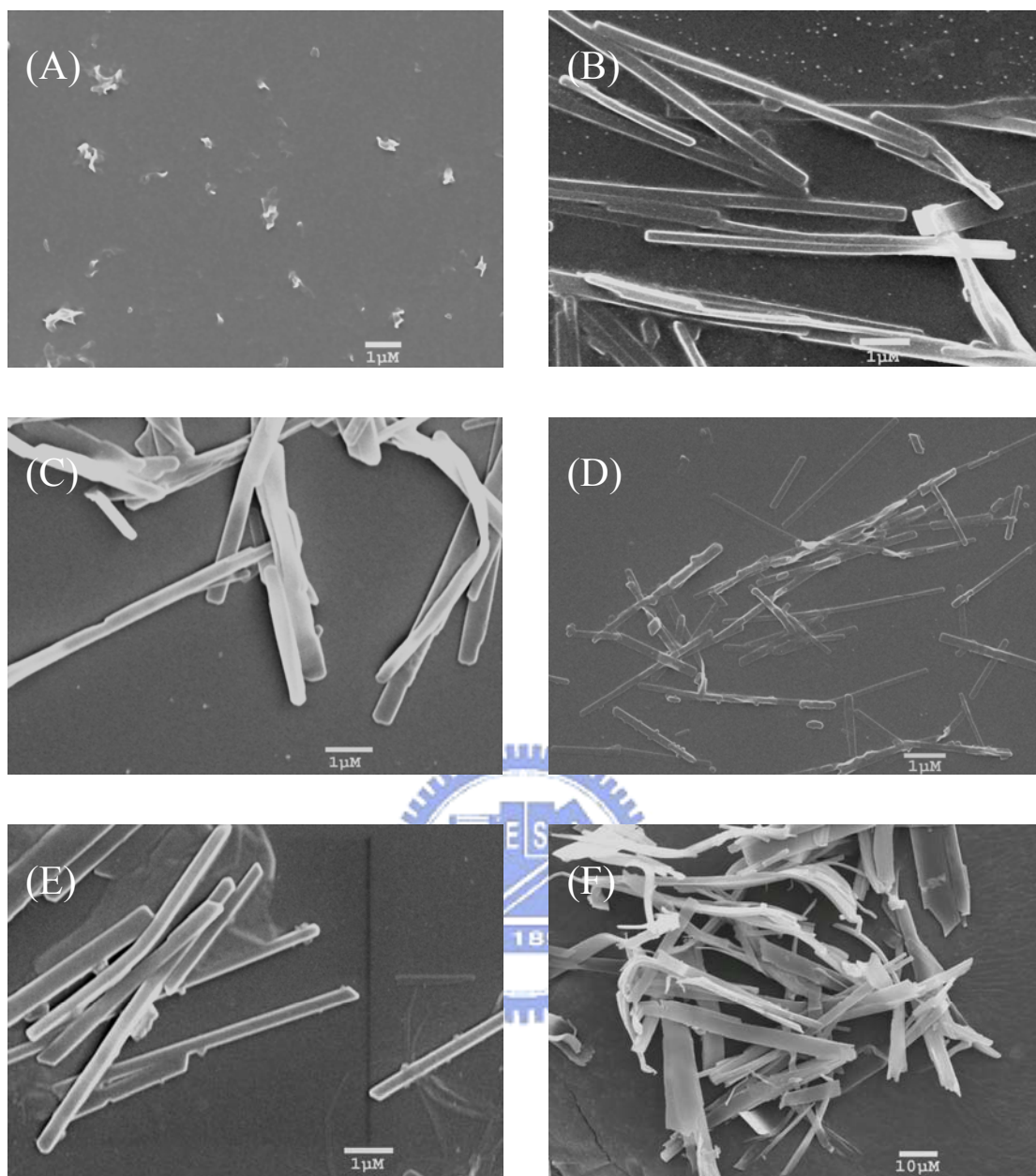[4] Yoshikava, H.; H., M. *J. Photochem. Photobiol., C* **2000**, 57.

Figure 4.1: SEM images showing the evolution of CN-DSB nanostrutures obtained at different water additions and at concentrations of 3.6×10^{-5} M. (A) 70, (B) 80, (C) 90% to THF, (D) 1.8×10^{-5} M for 80% solution, (E) 7.2×10^{-5} M for 80% solution, and (F) CN-DSB bulk crystals, respectively.

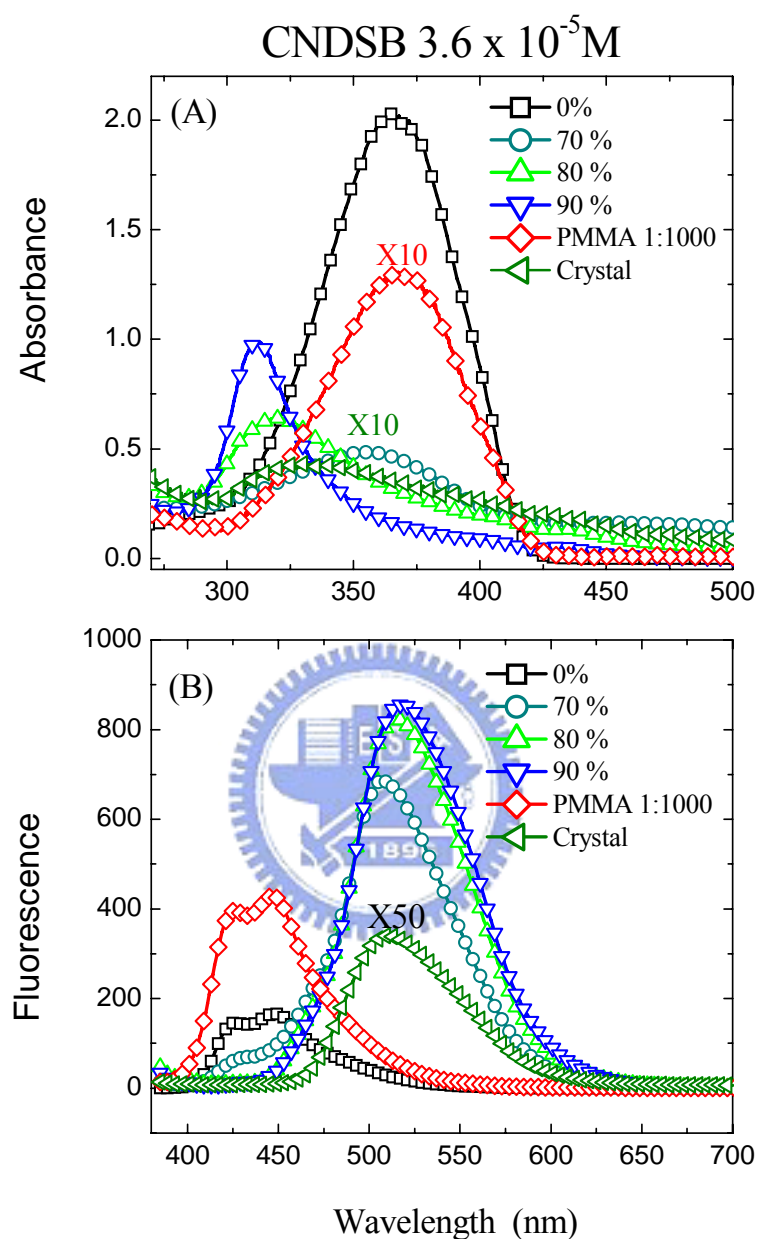**4.3.2 Steady-state Absorption/Emission Spectra**

CNDSB 3.6 x 10^{-5}M

Figure 4.2: (A) UV-visible spectra of CNDSB in various water/THF mixtures, the absorbance of PMMA and single crystal film were also indicated as red and olive symbols, respectively. (B) PL spectra of CNDSB in various percentages of water/THF solutions, PMMA thin film, and single crystal film.

CN-DSB is a greenish yellow solid at room temperature. In solution, it is almost non-fluorescent. Figure 4.2 shows the characteristic UV-visible absorption spectra (Figure 4.2A) and the corresponding emission spectra (Figure 4.2B) of CN-DSB with

various percentage of added water, CN-DSB single crystal, and CN-DSB in PMMA with the ratio of 1:1000.

The absorption spectra of CN-DSB in THF solution featured with a strong absorption maximum at 366 nm. When the percentage of water reaches 70%, the absorption is blue-shifted about 10 nm with a significant decrease of the absorbance. The hypsochromic shift in absorbance is attributed to the formation of the thin, curvy nanoparticles. With the water addition, dramatic changes are observed in the absorption spectra; The absorbance increases with a large blue shift from 366 nm to 320 nm (or 310 nm) for 80 % (or 90%) water/THF solutions, and the increasing of the baseline at longer wavelengths is due to the scattering of nanoparticles.[5] Since SEM image indicated that well-evolved nanobelts are formed in 80% and 90% water/THF solutions. This considerable increase of the absorbance and much significant blue shift are attributed to the formation of nanobelts. The blue-shifted nature of the absorption of CN-DSB nanobelts resembles that observed in DPST[6] and DSB,[7,8] in which substantially decreased emission intensity is reported on the formation of nanoparticles. In contrast, we observed the greatly fluorescence enhancement of CN-DSB nanobelts. Emission of CN-DSB in THF is very weak, and clear vibronic structures is observed around 425~445 nm (Figure 4.2B). At 70% solution, these vibronic structures almost disappear and giving rise to a red-shifted emission band (~505 nm) with enhanced emission intensity. At 80 and 90% volume fractions of

[5] Li, S.; He, L.; Xiong, F.; Li, Y.; Yang, G. *J. Phys. Chem. B* **2004**, *108*, 10887.
[6] An, B.-K.; Kwon, S.-K.; Jung, S.-D.; Park, S.-Y. *J. Am. Chem. Soc.* **2002**, *124*, 14410.
[7] Egelhaaf, H. J.; Gierschner, J.; Oelkrug, D. *Synthetic Metals* **1996**, *83*, 221.
[8] Oelkrug, D.; A., T.; Gierschner, J.; Egelhaaf, H.-J.; Hanack, M.; Hohloch, M.; Steinhuber, E. *J. Phys. Chem. B* **1998**, *102*, 1902.

water addition, a highly intense emission band was observed with a maximum peak at 518 nm; the observed intensity increases with the added water and consequently with the formation of well-evolved nanobelts. For the absorbance of single crystal, the powder of CNDSB single crystal is dispersed on quartz. The result indicates that the maximum shifted to ~340 nm, and the tail at long wavelength was attributed to the scattering of powder particles. The emission of CN-DSB single crystal showed maximum peak at about 510 nm, which was similar to CN-DSB nanobelts (70%, 80% and 90%). The similarity of absorption and emission spectra between CNDSB single crystal and nanobelt indicated that the packing of nanobelts is similar to the crystal one.

To investigate how intramolecular rotation or torsional motion affects the excited-state dynamics, we prepared the thin film of CN-DSB in PMMA (1:1000). The shape of absorption spectra (Figure 4.2A) was similar to the spectra of CNDSB in THF solution, indicated that no aggregation occurred in PMMA films. In PMMA film, the PL intensity was significant enhanced, which might due to the suppression of nonradiative decay in rigid environments, which proposed by Ran Yen *et. al.*[9,10] and we will discuss later.

4.3.3 Picosecond Relaxation Dynamics of CNDSB nanobelts

In Figure 4.3, ps time-resolved fluorescence spectra of CNDSB in water/THF solution were obtained using time-correlated single-photon counting (TCSPC) system. The excitation and probing wavelength was fixed at 375 and 500 nm, respectively.

[9] Ren, Y.; Dong, Y.; Lam, J. W. Y.; Tang, B. Z.; Wong, K. S. *Chem. Phys. Lett.* **2005**, *402*, 468.
[10] Ren, Y.; Lam, J. W. Y.; Dong, Y.; Tang, B. Z.; Wong, K. S. *J. Phys. Chem. B* **2005**, *109*, 1135.

Due to the limited temporal resolution of TCSPC, a sharp spike featured the transient of CNDSB in THF solution (0%). At 70% volume of water, additional long component appeared in the transient. This result is consistent with the fluorescence enhancement at 70% water/THF solution. In 70% solution, the SEM image indicated that CNDSB molecules start to aggregate to form curvy nanobelts, thus the slow component was attributed the emission of nanobelts. In 80% and 90% solution, the sharp spike disappear, the long component that appeared in 70% become the dominant part of the transient. This result indicates that most CNDSB molecules are aggregated, and the residual nonaggregate molecules are neglectable.
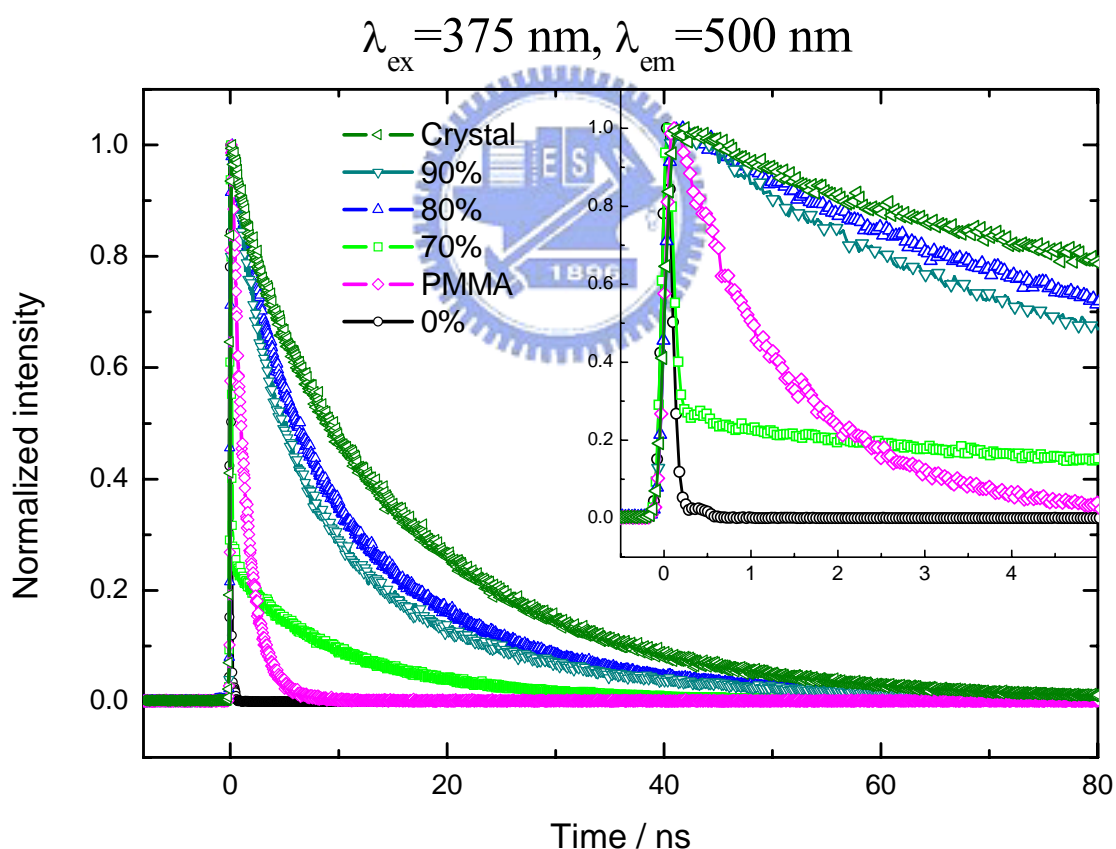

Figure 4.3: Picosecond time-resolved spectra of CNDSB in various water/THF mixtures, PMMA thin film, and single crystal obtained at λ_{ex}=375 nm, λ_{em}=500 nm. The inset was the corresponding transients in shorter time scale.

In order to avoid the interference from nonaggregate CNDSB molecules, we focused on the long decay components in 70%, 80%, and 90% solutions. Basically,

the transient can be fitted with a bi-exponential function:

$$A \xrightarrow{\tau_1} B$$
$$A' \xrightarrow{\tau_2} B' \tag{1}$$

The deconvolution of each component is shown in Figure 4.4.

For the assignment of A and A', we used the dual-emissive model, which we proposed previously in the study of PPB nanoparticles.[1] According to this model, two emissive states, intrinsic excitonic state and defect state exist in CNDSB nanobelts. For comparison, we measured the ps time-resolved transients of CNDSB single crystal. In Figure 4.4E, the transient of single crystal featured by a bi-exponential decay with τ_1=2.97 ns and τ_2=17.1 ns. Although τ_1 and τ_2 in single crystal are similar to that in nanobelts, the relative amplitude of τ_2 (or τ_1) differs from that in nanobelts. In signal crystal, the long component τ_2 became the dominant part of the transient. In 2003, with the application of femtosecond up-conversion microscopy, Tahara group measured the temporal resolved fluorescence transients of α -perylene microcrystal.[11] Their results indicated that the existence of the defect state in crystal would accelerate the fluorescence decay. It is reasonable for us to expect that the defects in single crystal are less than that in nanobelts. For above reason, the long component τ_2 in nanobelts or single crystal is attributed to the emission from the intrinsic excitonic state; the short component τ_1 is attributed to the emission of defect state.

---

[11] Fujino, T.; Tahara, T. *J. Phys. Chem. B* **2003**, *107*, 5120.

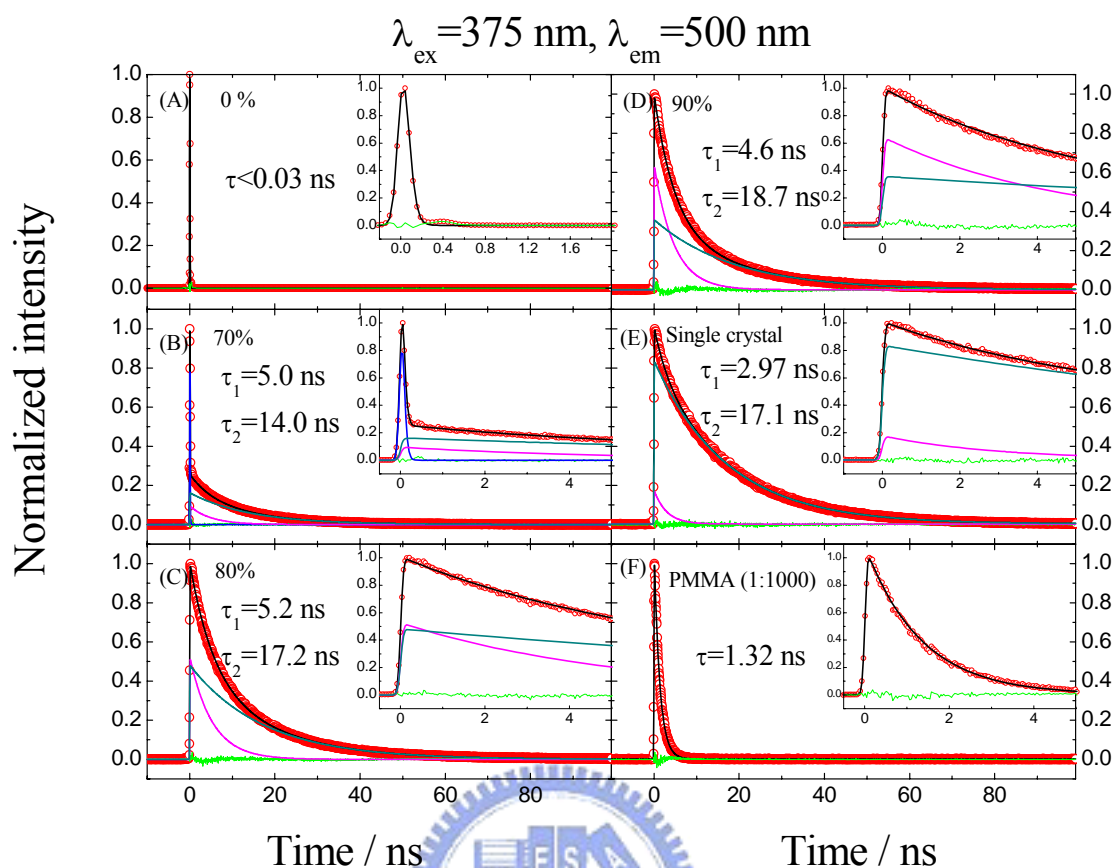λ_{ex}=375 nm, λ_{em}=500 nm

Figure 4.4: Picosecond transients of CNDSB in (A) 0%, (B) 70%, (C) 80%, (D) 90%, (E) single crystal, (F) PMMA film, each transients can be fitted with a bi-exponential function. The solid black curves are theoretical fits with residues shown as green traces; the short component was indicated as magenta line, and long component was indicated as dark cyan. The blue trace in 70% solution indicates the contribution from nonaggregate CNDSB molecules.

In Figure 4.4B, the observing τ_2 is shorter than that in 80%, 90% and single crystal. This is because the CNDSB molecules starts to aggregate to form nanoparticles at 70% solution, and the crystalline structure is not as good as those in higher percentage water/THF solutions or single crystal. The observing τ_2 is interfered by the defects in nanoparticles, thus caused the shorter lifetime we observed.

To investigate how intramolecular motion affects the excited state dynamics of CNDSB molecules, we measured the temporally resolved transients of CNDSB/PMMA films. In Figure 4.4F, the transients can be fitted by a

single-exponential decay with 1.32 ns time coefficient, which is much longer than that in THF, similar results were also observed by Yan Ren *et. al.*,[9,10] in which the lifetime of 1,1,2,3,4,5-hexaphenylsilole (HPS) increased significantly in high viscosity solvents and low-temperature glasses.

The UV and PL spectra of CNDSB in PMMA film are similar to that in THF solution. This result reveals that no aggregation and structural changes occurred in PMMA films. If the enhancement of the fluorescence quantum yield in nanobelt is only due to the structural confinement, the lifetime should close to that in PMMA film. However, in nanobelts, the lifetime is significant longer than that in PMMA films. This result indicated that structural confinement is not the only reason of fluorescence enhancement. The fluorescence enhancement in CNDSB nanobelts should contribute from both planar conformation and formation of aggregates, which has been discussed in our previous study.[1] Because of the limitation of temporally resolution, the ultrafast decay of CNDSB in THF solution could not be resolved by using TCSPC system. In order to get better understanding about the ultrafast processes, we measured the femtosecond time-resolved transients by fluorescence up-conversion technique, and the results would be shown in next section.

4.3.4 Femtosecond Relaxation dynamics of CNDSB in THF solution and

nanobelts

Figure 4.5A is the typical fluorescence transient of CNDSB in THF solution. With the application of femtosecond up-conversion technique, the pulse-limited component in

TCSPC system is resolved. The transient can be fitted by a bi-exponential decay with time coefficients of 0.9 ps and 24 ps. In trans-silbene, the nonradiative process in S_1 state is dominated by the isomerization along C=C bond with an energy barrier only 3.4 kJ mol^{-1}.[12] Considering the structural similarity between trans-stilbene and CNDSB, the observed 0.9 ps decay is attributed to the twisting along C=C coordinate, which leads to an efficient $S_1 \rightarrow S_0$ internal conversion channel at perpendicularly twisted conformation. This interpretation is supported by the result of CNDSB in PMMA film (Figure 4.5B), In PMMA film, the intramolecular motion is restricted, and the isomerization channel is energetically unfavorable because of the increasing of the energy barrier, therefore the sub-picosecond component is absent. Since the solvent molecules surround solute molecule, the importance of solvent-induced vibrational relaxation (VR) should be considered. In VR process, the excess vibrational energy of the excited molecules transfer to the surrounding molecules as heat, and relaxed to the lowest vibrational sub-level. In general, the time-scale of the vibrational cooling process ranges from tens of ps to sub-ps[13] depends on the excess energy and the type of solvent molecules.[14,15] For above reason, the observing 24 ps component is attributed to the vibrational cooling process.

[12] Felker, P. M.; Zewail, A. H. J. Phys. Chem. **1985**, 89, 5420

[13] Zewail, A. H. *J. Phys. Chem. A.* **2000**, *104*, 5660.

[14] Tan, X.; Gustafson, T. L. *J. Phys. Chem. A.* **2002**, *106*, 3593.

[15] Goldie, S. N.; Blanchard, G. J. *J. Phys. Chem. A* **2001**, *105*, 6785.
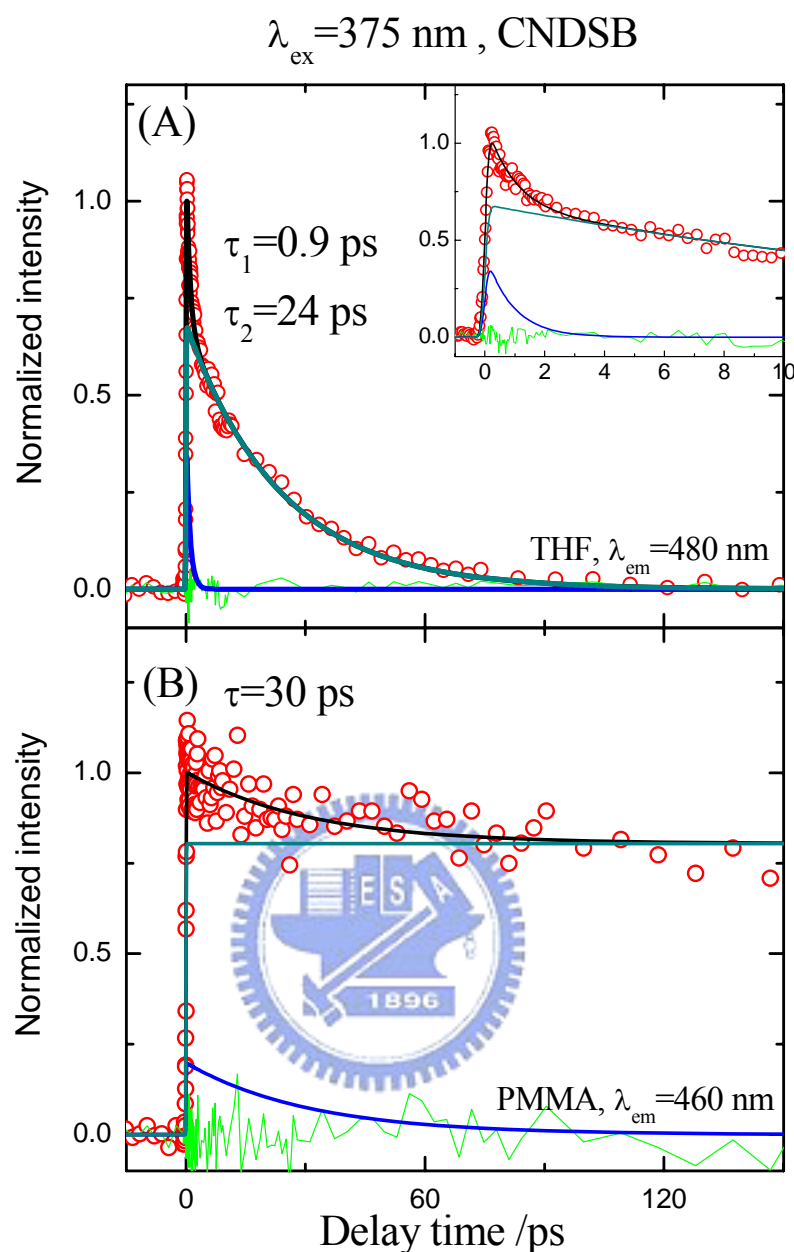
Figure 4.5: Femtosecond time-resolved spectra of CNDSB in (A) THF and (B) PMMA thin film. In each transient, the solid black curves are theoretical fits and the residues were shown as green trances. For THF solution, the transient was obtained at λ_{ex}=375 nm, λ_{em}=480 nm, and deconvoluted with bi-exponential function. The short component and long component were indicated as blue and dark cyan, respectively. For PMMA films, the transient was obtained at λ_{ex}=375 nm and λ_{em}=460 nm, and deconvoluted with bi-exponential function. The long component (dark cyan line) was fixed at the value obtaining from TCSPC technique.
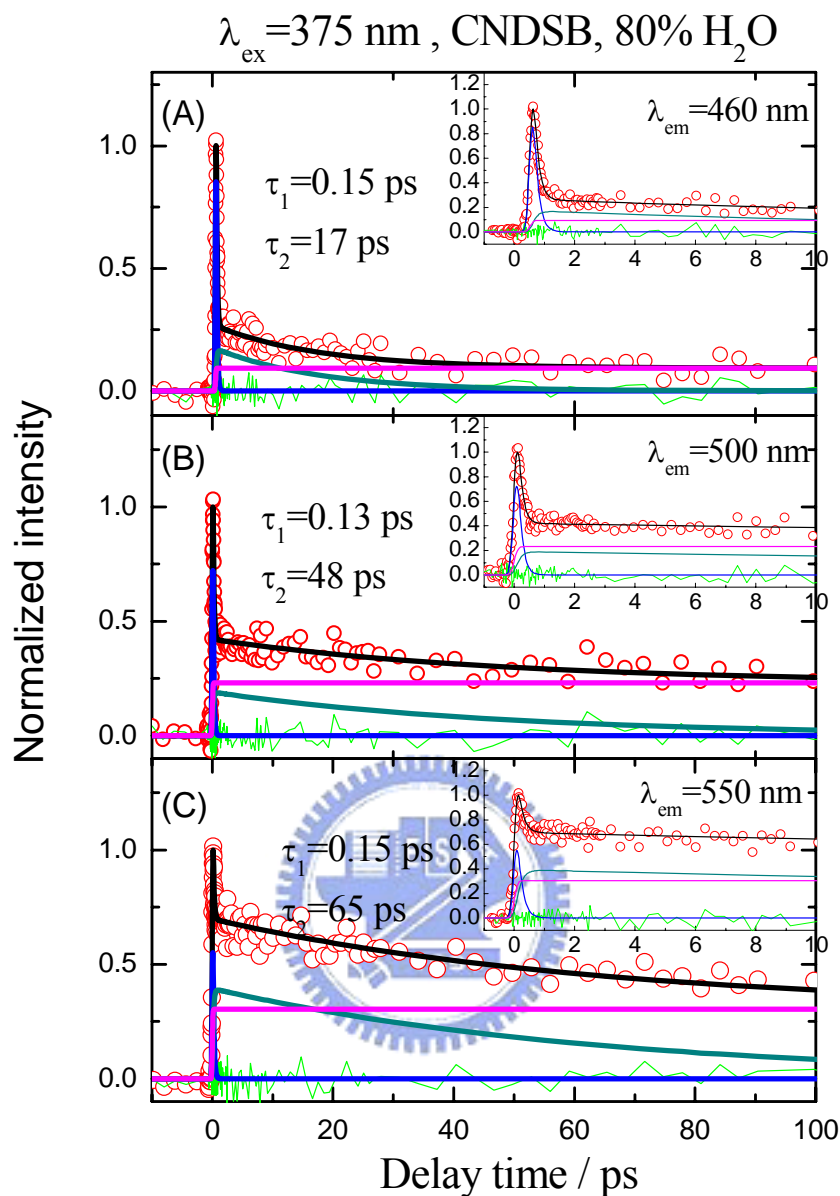
Figure 4.6: Femtosecond transients of CNDSB in 80% Water/THF solution, the excitation wavelength was fixed at 375 nm and probe at (A) 460 nm, (B) 500nm, (C) 550 nm. For each transient, at least three components were required to get the satisfactory fitting. The longest component (magenta line) was fixed at the value obtained from TCSPC result.

In Figure 4.5B the transient can be described with a 31 ps decay component, and an offset. Since similar energy transfer might also occur between CNDSB and PMMA polymer, the 30 ps component is attributed to the energy transfer process that occurred between CNDSB molecules and PMMA.

Figure 4.6 includes three typical fluorescence transients of CNDSB nanobelts probing at 460 nm, 500 nm, and 550 nm. In previous section, we have exam the fluorescence decay of CNDSB nanobelts in nanosecond time scale. In 0~100 ps range, the ns components become the offset in transient, and indicate as the magenta line. For the residual parts of the transient, a bi-exponential decay function is required to describe the transient. In generally, τ_1 is about 0.15 ps, which is wavelength independent. τ_2 varies from 17 ps to 65 ps and increases gradually with the detection wavelength. In previous study,[1] we measure the transients of PPB and DSB nanoparticles. The transient were dominated by a ~45 ps component, which was attributed to the nonradiative deactivation process through intermolecular interactions involving π -stacking of the carbon backbones. In CNDSB nanobelts, the τ_2 was attributed to the above mentioned energy transfer process, and the wavelength dependent feature indicated that this energy transfer process is more efficient for the molecules with more available energy. However, for nanobelts, an unusual ultrarapid process τ_1 is observed, which is absent in PPB and DSB nanoparticles. To verify the origin of this ultrafast component, a blank test has been done. We measured the fluorescence transient for 80% Water/THF solution at the same condition. The result (Figure 4.7A) indicated that the interference from the scattering light is small. In the other word, we also measure the fluorescence anisotropy spectra at λ_{ex}=375 nm and λ_{em}=500 nm. If the ultra-rapid component is the scattering light, r(0) should larger than 0.4, which is the theoretical value for the r(0),[16] and we should observe a pulse-limited component in anisotropy spectra.

---

[16] Lakowicz, J. R. *Principles of fluorescence spectroscopy*, 2 ed.; Kluwer Academic/ plenum: New York, 1999.

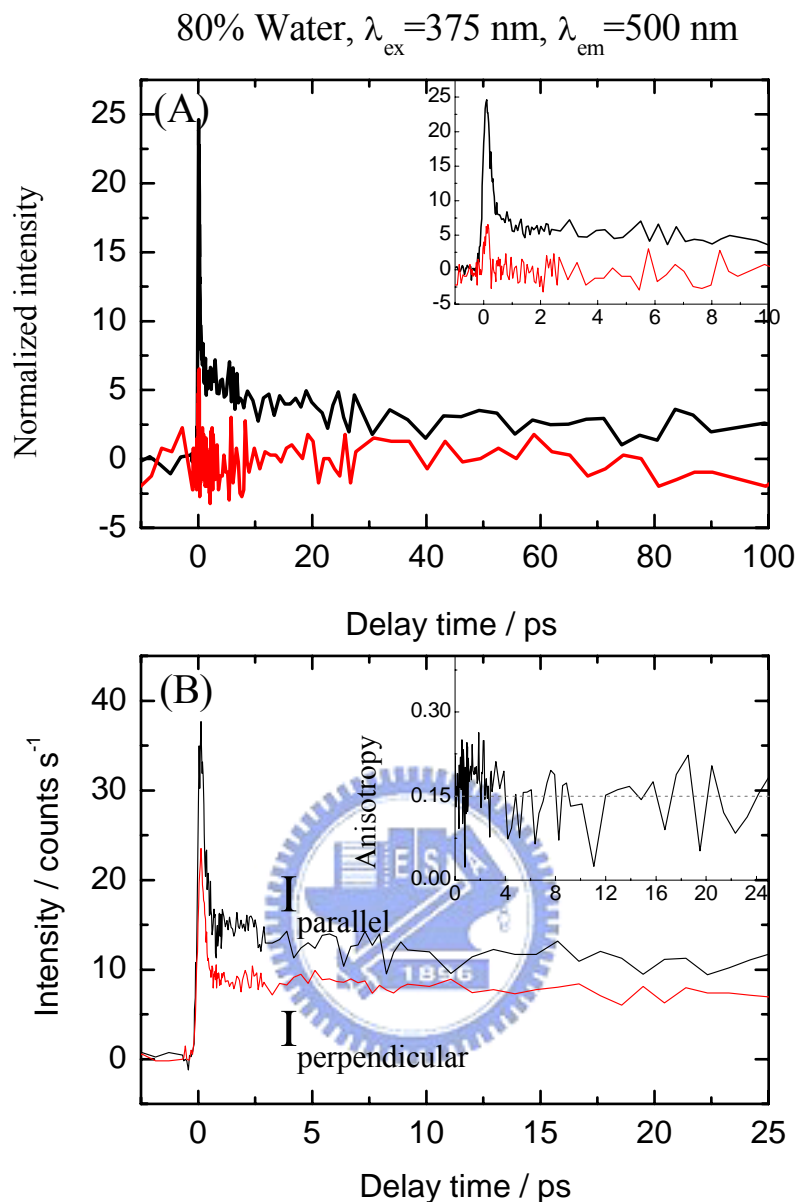80% Water, λ_{ex}=375 nm, λ_{em}=500 nm

Figure 4.7: (a) The blank test of CNDSB at 80% water/THF solution: The solid black line indicated the signal of CNDSB nanobelts, and the red line was the transient of 80% water/THF solution. (b) $I_{//}$ and $I\perp$ indicates the relative polarization of the collection fluorescence is parallel or perpendicular relative to the polarization of excitation beam. The anisotropy decay was calculated using the following equation:

$$r(t) = \frac{I_{//} - I_{\perp}}{I_{//} + 2I_{\perp}}$$

Since we did not observe any ultrafast decay in Figure 4.7B, the result supported

that the dynamic we observed is not the artificial effect. For nanoparticles, we only

observed a single exponential decay, and we attributed this decay to the

intermolecular energy transfer process. Since there is no preferred direction for the energy transfer, the rate we observed is the sum of the energy transfer through any direction. However, unlike the nanoparticle, nanobelt has it own crystal axis for the grown of crystalline structure. In nanobelts, the energy transfer is anisotropic along two axes. For above reason, the τ_1 and τ_2 were attributed the energy transfer through the long and short axis, respectively.

4.4 Concluding Remarks

In the present work, by comparing the time-resolved transients of CNDSB in THF and PMMA film, the excited state dynamic of CNDSB were investigated. For CNDSB in THF, both isomerization process (0.9 ps) and vibrational relaxation (24 ps) were observed. In PMMA film, because the isomerization channel was blocked, we only observed the energy transfer process (30 ps). For single crystal, the observed bi-exponential decay was attributed to the decay of intrinsic excitonic state (17.1 ns) and defect state (2.97 ns). The optical properties of CNDSB nanobelts were also investigated. The nanobelts were prepared by reprecipation methods and characterized by SEM, pico and femtosecond time-resolved spectroscopy. The SEM results indicated that CNDSB molecules formed nanobelts as the volume fraction of the water exceed 70%, and the size of the nanobelts increases with the increase of water. In this case, the size-dependence of fluorescence lifetime is not significant, and the dual-emissive model that we proposed previously can be used to explain the excited dynamics of nanobelts very well.

For CNDSB molecules, we provided the direct evidence of that the deactivation

through intramolecular isomerization channel. The result indicated that structural confinement only contributed parts of the fluorescence enhancement in nanobelts. Both the planar conformation and formation of aggregates in nanobelts contribute parts of the fluorescence enhancement. The result of femtosecond time-resolved fluorescence spectroscopy indicated that a unique ultra-fast energy transfer process existed in CNDSB nanobelts, which is absent in nanoparticles.